



# On the Role of Air Flow in Air-Convection Embankments: Insights from Thermal Numerical Modeling

Ahmed Ibrahim<sup>(✉)</sup> and Mohamed A. Meguid

McGill University, Montreal, QC, Canada  
ahmed.ibrahim5@mail.mcgill.ca

**Abstract.** Utilizing crushed rocks in air convection embankments is one of the methods adopted to facilitate heat exchange between foundation soil and the atmosphere. The relatively large pore space provided by the air convection section allows for air to overall decrease the temperature of permafrost underneath the embankment. As air flow is the main component in this approach, coupled air flow-thermal conduction has been adopted to numerically simulate the temperature distribution in air convection embankments. Such coupling, however, can be computationally expensive and rather complicated to perform. Considering the bulk thermal characteristics of air convection sections, we explore the potential of pure conduction models to model such systems. The results show a good agreement between pure conduction results, experimental data, and coupled analysis. The slight deviation of the simulation results from both experimental and coupled analysis suggests a minimal contribution of the air flow portion of previous models. The preliminary results presented in this paper indicate that pure conduction non-coupled models can be a viable, simple, and effective approach for the thermal modeling of air convection embankments.

**Keywords:** Air-convection embankments · permafrost · numerical modeling

## 1 Introduction

Under a constantly changing climate, embankments built on permafrost soils are increasingly more prone to failure. As the pore ice within the foundation soil thaws, the shear strength of the foundation soil is reduced imposing different sorts of structural damage to embankments that can potentially cause total failure. This issue is further magnified in the northern regions where the rate of warming is nearly double that of the average. Different techniques have been adopted to maintain the permafrost underneath the embankment such as thermosyphons, slope shading, and air convection shoulders and bodies [1–4]. The experimental site of Beaver’s Creek provides some valuable data on the efficiency of such methods.

Among the methods that provided significant improvement of reducing the temperature of the permafrost region is using air-convection embankments. Air convection is basically achieved by introducing a portion of crushed rock of high permeability into

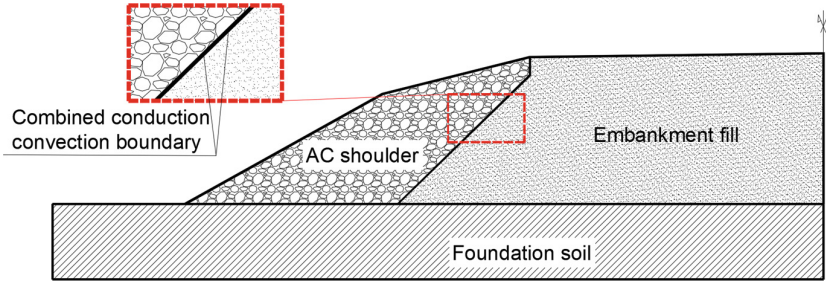


**Fig. 1.** Schematic of air convection shoulder embankment

the body or the shoulders of the embankment. Through this layer, air flow into the embankment is facilitated, enhancing the foundation soil's cooling process. Numerical modeling has been conducted to develop and calibrate models for simulating air convection embankments. Kong et al. [5] presented a coupled air heat convection and heat conduction model to simulate the coupled effect of conduction and convection.

Such a modeling approach, however, raises a question about the effect of air flow on cooling the permafrost layer. Since air velocity gradients are relatively small compared to other conduction terms, the contribution momentum-dependent would be marginal and the main convection contribution would be density-driven. Considering the drastic change in the thermal properties resulting from introducing the air convection section, it is difficult to conclude, without proper quantification, the role of air flow in the cooling process. Indeed, the contact between the pore space air and the adjacent embankment fill can contribute to the thermal balance through convection. This, however, will be done through a limited area where air convection rocks are not in direct contact with the embankment fill or the subgrade (Fig. 1). As such, we here explore the contribution of air flow portion of the modeling by comparing field measurements and coupled air flow-conduction analysis with a pure conduction finite element model. This comparison should not only help quantify the air flow effect, but also shed light on the optimal approach for modeling air convection embankments.

## 2 Numerical Modeling

In this section we carry out thermal numerical modeling of air-convection shoulder embankment following the work of Kong et al. [5] as shown in Fig. 2. The modeling case is solely based on conductive heat transfer between the different parts of the embankment as well as the foundation soil. The reason we only consider conduction here is to role out the effect of air flow within the air convection part. Neglecting the effect of groundwater flow, the conductive heat transfer within the different parts of the embankment is expressed as:

$$\frac{\partial}{\partial x} \left( k_x \frac{\partial T}{\partial x} \right) + \frac{\partial}{\partial y} \left( k_y \frac{\partial T}{\partial y} \right) = C \frac{\partial T}{\partial t} - L_f \frac{\rho_i}{\rho_w} \frac{\partial \theta_i}{\partial t} \quad (1)$$

where  $k_x$  is the thermal conductivity in  $x$  direction,  $k_y$  is the thermal conductivity in  $y$  direction,  $T$  is temperature,  $C$  is the volumetric heat capacity,  $L_f$  the volumetric latent heat of fusion of water,  $\rho_i$  is the density of ice,  $\rho_w$  is the density of water, and  $\theta_i$  the unfrozen water content. The dimensions of the embankment considered for the simulation case is shown in Fig. 2. The thermal properties of embankment fill, crushed rocks, and subgrade soil are shown in Table 1.

A time-dependent temperature boundary condition is imposed on the outermost surface including the top of the embankment, shoulder, and the exposed ground surface in the vicinity. The value of the temperature boundary condition is developed from the surrounding air temperature from January 2009 to January 2014 (Fig. 3).

Heat transfer from the surrounding air to the adjacent soil or rock is modified by the  $n$  factor which represents the ratio between the soil average temperature compared to that of the surrounding air. As the value of the  $n$  factor depends on the material type, different  $n$  factors have been assigned for the three different types of materials and the state of freezing/thawing (Table 2). At the far bottom end of the computational domain, located 30 m beneath the ground surface, heat flux of  $0.03 \text{ W/m}^2$  is applied to simulated the increase of temperature due to geothermal energy gradient.

The modeling was carried out using RS2 software for two-dimensional finite element computations.

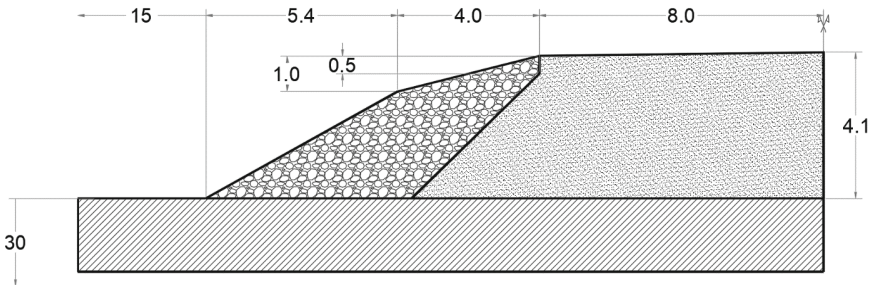


**Fig. 2.** Dimensions (m) of the air convection shoulder embankment considered for numerical analysis (adapted from Kong et al. [5])

**Table 1.** Material properties for different parts of the embankment and subgrade soil

Material type	$k_f$ (W/m-°C)	$k_u$ (W/m-°C)	$C_f$ (MJ/m <sup>3</sup> -°C)	$C_u$ (MJ/m <sup>3</sup> -°C)	K (m <sup>2</sup> )
Rock layer	0.35	0.35	1.098	1.098	$6 \times 10^{-7}$
Fill	1.134	1.443	1.43	1.58	$\approx 0$
Subgrade	1.337	1.337	1.73	2.51	$\approx 0$

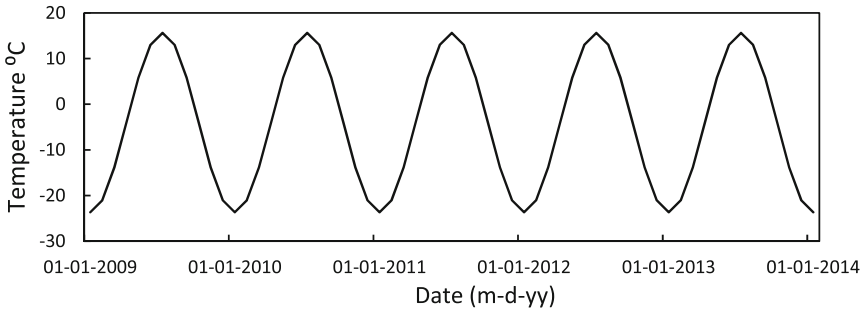


**Fig. 3.** Air temperature (°C) at the embankment site from January 2009 to January 2014

**Table 2.** Factors for the embankment body and subgrade soil

Surface type	$n_t$	$n_f$
Natural ground surface	0.37	0.29
Embankment surface	1.6	1
Embankment side slopes	1.05	0.6

### 3 Results

The simulation results for temperature distribution over depth was determined for two control sections; under the centerline of the embankment and the air convection shoulder. The results shown in Fig. 4 show the simulated temperature distribution on January 1<sup>st</sup> 2012 and July 1<sup>st</sup> 2012 at the centerline of the embankment. It can be seen that the results from the pure conductive simulation align decently with the reported experimental measurements as well as the coupled air flow-conduction simulation. There is, however, a deviation in the results that reaches up to 5% of the results which may be attributed to the effect of air flow. It is also observed that the pure conduction results result in warmer predictions in winter while in summer the predicted temperatures are slightly lower than measured. This, again, can be attributed to the role of air convection that was not considered in the simulation. As a result, the pure conduction simulation is slightly deviated from the measured data. However, the fact that this deviation is minimal suggests that the bulk change in the thermal properties such as thermal conductivity and heat capacity of the air convection portion is dominant over the air flow mechanism. Interestingly, both coupled and pure conduction models are nearly equally deviated from the experimental measurements on July 1<sup>st</sup> at both measurement sections. Although it is not conclusive as to what may be the reason behind this, the general trend and conclusions regarding the contribution of air flow remain the same. The same insights can be drawn from the simulation results at the section located beneath the air convection shoulder (Fig. 5). These conclusions remain pertinent to preliminary analysis and it require further quantification of the contribution of air flow on the thermal analysis in order to support these results (Fig. 6).

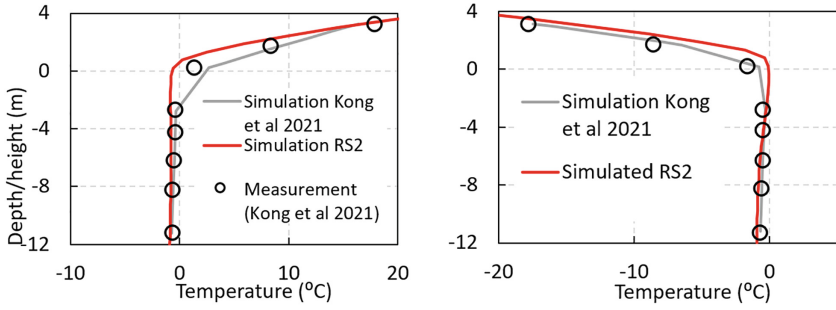


**Fig. 4.** A comparison between conduction and coupled simulation with the experimentally measured temperature distribution along the centerline of the embankment on July 2012 (left) and January 2012 (right)

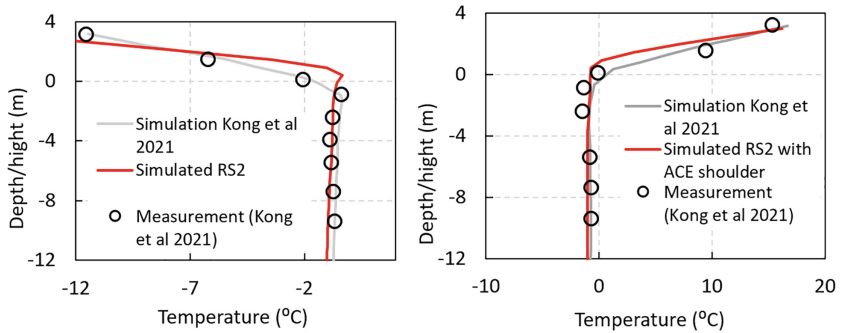


**Fig. 5.** A comparison between conduction and coupled simulation with the experimentally measured temperature distribution along the shoulder of the embankment on July 2012 (right) and January 2012 (left)

### 4 Discussion

To further quantify the contribution of air flow we need to give a closer look on the air flow equations within the air convection layer. The energy equation combining convective and conductive heat transfer can be expressed as:

$$\frac{\partial}{\partial x} \left( k_x \frac{\partial T}{\partial x} \right) + \frac{\partial}{\partial y} \left( k_y \frac{\partial T}{\partial y} \right) - C_a \left( v_x \frac{\partial T}{\partial x} + v_y \frac{\partial T}{\partial y} \right) = C \frac{\partial T}{\partial t} \tag{2}$$

where  $C_a$  is the volumetric heat capacity of air and  $v_x$  and  $v_y$  are the air flow velocities in  $x$  and  $y$  directions. Now, considering the air flow equations for  $v_y$ :

$$v_y = -\frac{K}{\mu} \bullet \left( \frac{\partial P}{\partial y} + \rho_a g \right) \tag{3}$$

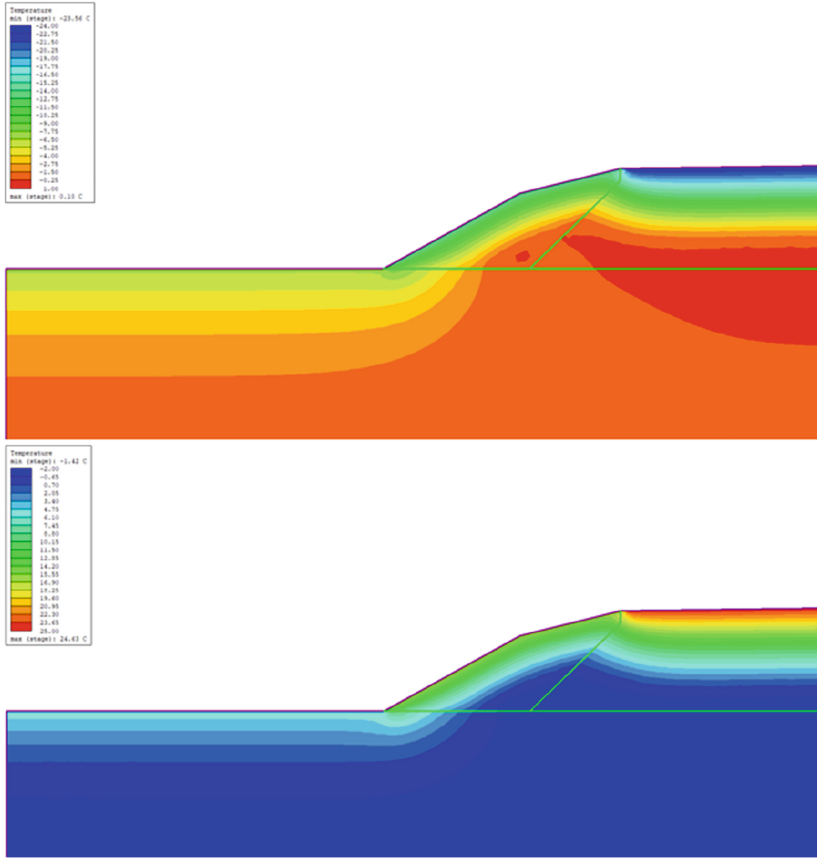


**Fig. 6.** Temperature distribution within the embankment and foundation soil in January 2012 (top) and July 2012 (bottom)

where  $K$  is the intrinsic permeability of the air convection layer,  $\mu$  is the kinematic viscosity of air,  $P$  is air pressure inside the air convection layer, and  $\rho_a$  is the air density. Similarly in  $x$  direction:

$$v_x = -\frac{K}{\mu} \cdot \frac{\partial P}{\partial x} \tag{4}$$

To simplify the problem, we assume that the air convection is exclusively density driven (natural convection). Therefore, the pressure distribution in both  $x$  and  $y$  directions can be assumed uniform, which makes the velocity component in  $x$  direction nearly negligible. In  $y$  direction, considering that the medium temperature is approximately uniform, the relationship between air density and temperature is given as:

$$\rho_a = \rho_0[1 - \beta(T - T_0)] \tag{5}$$

Considering the velocity  $v_y$  from Eq. 3 incorporating the relationship in Eq. 5, we can write the velocity gradient as:

$$v_y = -\frac{K}{\mu}(\rho_0 g [1 - \beta(T - T_0)]) \quad (6)$$

From Eq. 6, the convection term in Eq. 2 can be rewritten as:  $C_a \frac{K}{\mu} (\rho_0 g [1 - \beta(T - T_0)]) \frac{\partial T}{\partial y}$ . This expression is quantifiable except for the temperature gradient which is one of the outputs of the model. Nonetheless, one can still estimate the portion of convection contribution as a ratio to  $\partial T / \partial y$ , for which the simulated temperatures may be considered a reasonable approximation. By incorporating some typical values for the involved parameters:  $C_a = 1.2 \text{ kJ}/(\text{m}^3 \cdot \text{C})$ ,  $K = 6 \times 10^{-7} \text{ m}^2$ ,  $\mu = 1.4 \times 10^{-5} \text{ (m}^2\text{s}^{-1})$ ,  $\rho_0 = 1.204 \text{ kg}/\text{m}^3$ , and  $\beta = 0.00369 \text{ (1/K)}$ , the contribution of the convection term ranges between 0.015 to 0.021 of  $\partial T / \partial y$ . When this evaluation is coupled with the contribution of conduction in Eq. 1, the deviation of the conduction results can be justified. We note, however, that considering conduction and air convection as two separate contributors does not closely represent reality nor should it be the ideal modeling approach. Therefore, some of the discrepancies cannot be explained in such separative framework, instead, the two-way coupling effect needs to be considered.

## 5 Conclusions

In this paper we briefly investigated the potential of pure conduction models to simulate air convection embankments. The simulation case considered tackled an embankment with air convection shoulder layer. The results from pure conduction model were compared with both more refined coupled analysis and experimental measurements. The comparison showed a decent agreement between the conducted simulation and previously presented experimental and numerical results. Some discrepancies were observed between the coupled air convection-conduction model and the pure conduction model which we attribute to the role of air flow. The fact that these discrepancies are minor indicates that the bulk change in the thermal properties of the air convection layer is more effective to the cooling process than the air flow mechanism within the air convection layer. In addition, an attempt to quantify the contribution of air flow through natural convection to the overall energy balance. The preliminary calculations show that the convection contribution to the overall thermal gradient is relatively small. In conclusion, the presented results demonstrate the potential of pure conduction model as a computationally effective and less complicated, yet effective, modeling approach for air convection embankments.

**Acknowledgement.** The Authors would like to like to acknowledge the funding and software provided by Rocscience.

## References

1. M-Lepage J, Dore G, Fortier D (2012) Thermal effectiveness of the mitigation techniques tested at Beaver Creek Experimental road site based on a heat balance analysis (Yukon, Canada). Paper presented at the 15th International Conference on Cold Regions Engineering, Quebec, Canada.
2. Darrow MM, Jensen DD (2016) Modeling the performance of an air convection embankment (ACE) with thermal berm over ice-rich permafrost, Lost Chicken Creek, Alaska. *Cold Reg Sci Technol* 130:43–58. doi:<https://doi.org/10.1016/j.coldregions.2016.07.012>
3. Lai YM, Wang QS, Niu FJ, Zhang KH (2004) Three-dimensional nonlinear analysis for temperature characteristic of ventilated embankment in permafrost regions. *Cold Reg Sci Technol* 38 (2–3):165–184. doi:<https://doi.org/10.1016/j.coldregions.2003.10.006>
4. Zhang MY, Pei WS, Li SY, Lu JG, Jin L (2017) Experimental and numerical analyses of the thermo-mechanical stability of an embankment with shady and sunny slopes in a permafrost region. *Appl Therm Eng* 127:1478–1487. doi:<https://doi.org/10.1016/j.applthermaleng.2017.08.074>
5. Kong XB, Dore G, Calmels F, Lemieux C (2021) Field and numerical studies on the thermal performance of air convection embankments to protect side slopes in permafrost environments. *Cold Reg Sci Technol* 189:103325. doi:<https://doi.org/10.1016/j.coldregions.2021.103325>

**Open Access** This chapter is licensed under the terms of the Creative Commons Attribution-NonCommercial 4.0 International License (<http://creativecommons.org/licenses/by-nc/4.0/>), which permits any noncommercial use, sharing, adaptation, distribution and reproduction in any medium or format, as long as you give appropriate credit to the original author(s) and the source, provide a link to the Creative Commons license and indicate if changes were made.

The images or other third party material in this chapter are included in the chapter's Creative Commons license, unless indicated otherwise in a credit line to the material. If material is not included in the chapter's Creative Commons license and your intended use is not permitted by statutory regulation or exceeds the permitted use, you will need to obtain permission directly from the copyright holder.

